Nano Research 2014, 7(9): 1327–1336
DOI 10.1007/s12274-014-0497-9
Research Article
ISSN 1998-0124
CN 11-5974/O4

Aptamer-conjugated upconversion nanoprobes assisted by magnetic separation for effective isolation and sensitive detection of circulating tumor cells

Shuai Fang[§], Chao Wang[§], Jian Xiang, Liang Cheng, Xuejiao Song, Ligeng Xu, Rui Peng (✉), and Zhuang Liu (✉)

Institute of Functional Nano & Soft Materials (FUNSOM), Collaborative Innovation Center of Suzhou Nano Science and Technology, Soochow University, Suzhou, Jiangsu 215123, China
[§] *These two authors contributed equally to this work.*

Received: 15 April 2014
Revised: 9 May 2014
Accepted: 12 May 2014

KEYWORDS
circulating tumar cell (CTC) detection,
upconversion nanoparticles,
magnetic nanoparticles,
aptamer

ABSTRACT

Detection of circulating tumor cells (CTCs) plays an important role in cancer diagnosis and prognosis. In this study, aptamer-conjugated upconversion nanoparticles (UCNPs) are used for the first time as nanoprobes to recognize tumor cells, which are then enriched by attaching with magnetic nanoparticles (MNPs) and placing in the presence of a magnetic field. Owing to the autofluorescence-free nature of upconversion luminescence imaging, as well as the use of magnetic separation to further reduce background signals, our technique allows for highly sensitive detection and collection of small numbers of tumor cells spiked into healthy blood samples, and shows promise for CTC detection in medical diagnostics.

1 Introduction

Circulating tumor cells (CTCs) [1] shed from the primary tumor into bloodstream are an important indication of cancer metastasis [2, 3]. Their effective capture and detection are therefore of great importance in cancer diagnosis and prognosis. At present, CellSearch® is the only medical device certificated by the US Food and Drug Administration (FDA) for CTC detection in the clinic [4]. This technique, however, requires expensive instruments and is rather time consuming. In recent years, tremendous efforts have been devoted to the development of new CTC capture and detection techniques [5–13], many of which are based on nanotechnology employing a variety of different mechanisms. However, due to the extraordinarily small number of CTCs in the blood of cancer patients (one in 10^6 hematologic cells) [14], the

Address correspondence to Zhuang Liu, zliu@suda.edu.cn; Rui Peng, rpeng@suda.edu.cn

development of new CTC detection technology that is easy to operate and highly sensitive still merits further exploration.

Upconversion nanoparticles (UCNPs), which are typically nanocrystals containing lanthanide ions, have emerged as a unique class of optical nanoprobes that under excitation by multiple low-energy near-infrared (NIR) photons can emit a high-energy photon at a shorter wavelength [15, 16]. In the past few years many groups, including ours, have explored the biomedical uses of UCNPs for biological sensing, imaging and even therapy, by taking advantage of the interesting upconversion phenomena of such nanoparticles [17–23]. While autofluorescence background is usually the major factor that limits the sensitivity of conventional down-conversion fluorescence imaging, one of the most important advantages of UCNPs is the autofluorescence-free nature of upconversion luminescence (UCL) imaging, enabling imaging in biological samples with very high sensitivity [24–26]. In our recent studies, we have demonstrated the ultra-high *in vivo* tracking sensitivity of UCNP-labeled stem cells down to the single cell level in mice [27, 28]. Therefore, we wonder if UCNP-based CTC detection, which has not yet been demonstrated by others to our best knowledge, would have any potential.

In this work, we develop a novel CTC detection method by combining aptamer-conjugated UCNPs for tumor cell targeting and iron oxide magnetic nanoparticles (MNPs) for magnetic separation. In this strategy, tumor cells are first specifically recognized by aptamer/biotin co-conjugated UCNPs (UCNP–Apt–Biotin), which are then captured by avidin-conjugated MNPs (MNP–Av) (Fig. 1(a)). After magnetic separation, UCL imaging is conducted to detect the positive tumor cells spiked into large numbers of negative cells or even healthy human blood samples. As the result of the autofluorescence-free characteristics of UCL imaging, as well as the reduced non-specific signals after magnetic separation, our approach—which is a rather simple one—enables highly sensitive detection of small numbers of tumor cells in an ocean of negative cells, or even in whole blood samples, and shows promise for future applications in CTC detection for cancer diagnosis.

2 Experimental

2.1 Materials

Y_2O_3, Yb_2O_3, Er_2O_3 and CF_3COOH were purchased from Shanghai Chemical Industrial Co. Oleic acid (OA, >90%) and 1-octadecene (ODE, >90%) were purchased from Sigma-Aldrich.

2.2 Synthesis of UCNPs

UCNPs were prepared according to previous literature protocol [29]. Typically, 1 mmol of Re $(CF_3COO)_3$ (Y:Yb:Er = 78%:20%:2%), 20 mmol of NaF, 10 mL of OA and 10 mL of ODE were simultaneously added to a 100-mL three-necked flask, and then degassed at 100 ℃ for 1 h under vacuum. Afterwards, the mixture was rapidly heated to 320 ℃ and kept at this temperature under vigorous magnetic stirring for 30 min in the presence of nitrogen. After cooling down to the room temperature, the product was precipitated by addition of ethanol, separated by centrifugation, washed by cyclohexane and ethanol for purification. The as-made nanoparticles could be easily re-dispersed in chloroform for further modification.

2.3 PEGylation of UCNPs

Amine-terminated polyethylene glycol (PEG)-grafted poly(maleic anhydride-alt-1-octadecene) (C_{18}PMH–PEG–NH_2) polymer was synthesized according to previous reports [30]. 500 μL of UCNPs stock solution in chloroform was mixed with 5 mg of C_{18}PMH–PEG–NH_2 polymer in 2 mL of chloroform. After stirring at room temperature for 2 h, chloroform was blow-dried. The leftover residue was dissolved in water and then filtered through a 0.22-mm syringe filter to remove large aggregates. The obtained PEGylated UCNPs (UCNP–PEG–NH_2) were kept at 4 ℃ for following experiments

2.4 Aptamer conjugation to UCNPs

Thiol-modified aptamer with a sequence of 5′-thiol-TTTTTTTTTTATCTAACTGCTGCGCGCCGGGAAAATACTGTACGGTTAGA was purchased from TakaRa. UCNP–Apt–Biotin was synthesized according to a similar procedure to that used for protamine labeling

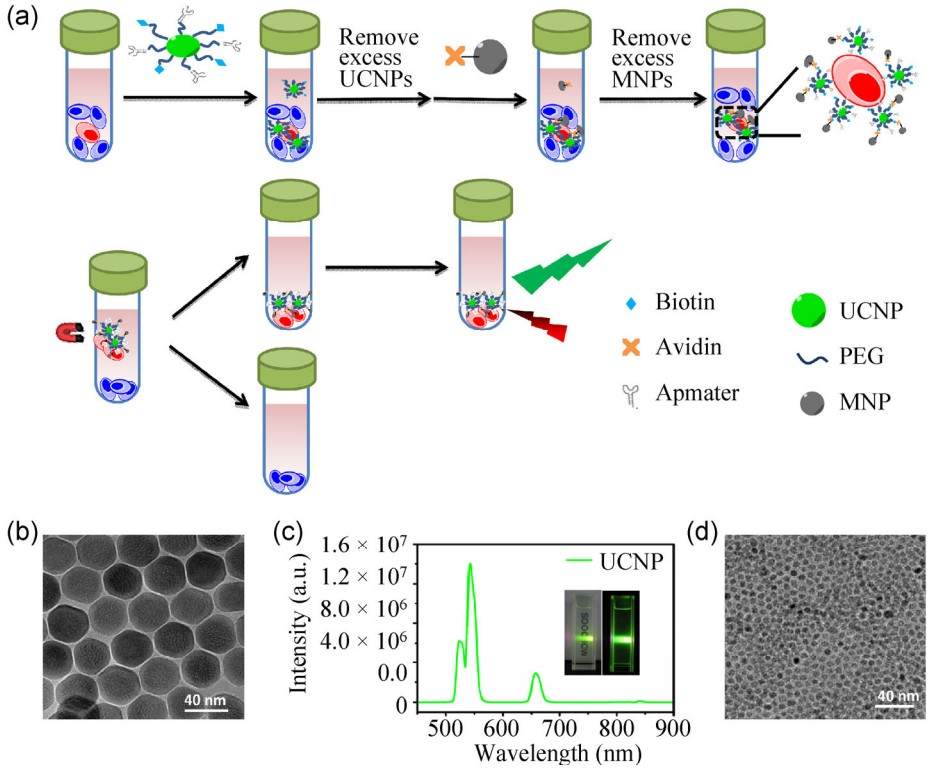

Figure 1 (a) Schematic illustration of using UCNP–Apt–Biotin and MNP–Av nanoprobes for CTCs detection. Positive tumor cells are recognized by UCNP–Apt–Biotin nanoprobes, which are then specifically attached by MNP–Av nanoparticles for magnetic separation. The UCL signals from UCNPs could be utilized for tumor cell detection. (b) A TEM image of as-made UCNPs ($NaYF_4$: 78% Y, 20% Yb, 2% Er). (c) Upconversion luminescence spectrum of PEGylated UCNPs in an aqueous solution. Inset: a photograph of a UCNP aqueous solution excited by a 980-nm laser. (d) A TEM image of as-made MNPs.

in our previous work [31]. Firstly, UCNP–PEG–NH_2 (0.5 mg·mL^{-1}) was mixed with sulfosuccinimidyl-4-(*N*-maleimidomethyl) cyclohexane-1-carboxylate (sulfo-SMCC, Pierce) (1 mg·mL^{-1}) and sulfosuccinimidyl-6-[biotin-amide]hexanoate (sulfo–NHS-LC–biotin) (Pierce) (1 mg·mL^{-1}) in phosphate buffered saline (PBS, pH 7.4). After reaction for 2 h, excess sulfo-SMCC and sulfo–NHS-LC–biotin were removed by centrifugation and water washing. Afterwards, the SMCC- activated and biotinylated UCNPs and aptamer-SH was mixed in PBS (pH 7.4) at a molar ratio of sulfo- SMCC:aptamer = 1:5. After reaction for 24 h at 4 ℃, excess aptamer was removed by centrifugation. The obtained UCNP–PEG–aptamer–biotin was stored at 4 ℃ for further experiments.

2.5 Synthesis of Fe_3O_4 MNPs and subsequent Av conjugation

Fe_3O_4 MNPs were synthesized from iron(III) acetylacetonate ($Fe(acac)_3$) based on a well-established method [32]. To modified as-made MNPs [33], 20 mg of meso-2,3-dimercaptosuccinic acid (DMSA, Sigma-Aldrich) was dissolved in 1 mL of water containing Na_2CO_3, and then slowly added into a tetrahydrofuran (THF) solution containing 20 mg of MNPs under ultrasonication for 30 min. After further stirring at room temperature for 2 h, the DMSA-modified iron oxide nanoparticles (IONPs) (MNP–DMSA) were collected by centrifugation and could be re-dispersed in water with excellent stability.

To conjugate Av (Pierce) to MNPs, MNP–DMSA (1 mg·mL^{-1}) was mixed with 2 mM 1-(3-dimethylamino-propyl)-3-ethylcarbodiimide hydrochloride (EDC) and 5 mM sulfo-*N*-hydroxysuccinimide (sulfo-NHS) in PBS (0.1 M, pH 6.5) for 30 min at room temperature (RT). Av (1 mg·mL^{-1}) was then added to the activated MNP sample and reacted for 2 h in PBS (0.1 M, pH 7.5) at room temperature. Finally, the obtained MNP–Av conjugate was purified by centrifugation at 14,800 rpm for 10 min.

2.6 Cell culture

CCRF-CEM cells (CCL-119 T-cell, human acute lymphoblastic leukemia) and human erythroleukemia K562 cells were obtained from American Type Culture Collection (ATCC). Cells were grown in RPMI 1640 medium supplemented with 10% fetal bovine serum (FBS) and 1% penicillin/streptomycin in a humidified atmosphere containing 5% CO_2 at 37 ℃.

2.7 Cell labeling by UCNPs and MNPs

To evaluate the specificity of UCNP–Apt–Biotin nanoprobes to CCRF-CEM and K562 cells, UCNP–Apt–Biotin (0.2 mg·mL^{-1}) was separately added into 500 μL of PBS (0.01 M, pH 7.4) containing 0, 10, 50, 100, 500 and 1,000 CCRF-CEM cells or K562 cells, respectively. After incubation for 2 h at 4 ℃, the cells were washed three times with PBS using centrifugation to remove excess nanoparticles. The collected cells were re-dispersed in 100 μL of PBS in a 1.5-mL tube and then imaged by using a modified Maestro *in vivo* imaging system (CRiInc) using a 980-nm optical fiber-coupled laser (Hi-Tech optoelectronics Co., Ltd) as the excitation source. An 850 nm short-pass emission filter was applied to prevent the interference of excitation light with the CCD camera. The laser power density was ~1.5 W·cm^{-2} during imaging with an exposure time of 15 s. The UCL intensity of each sample was analyzed by the Maestro software.

To estimate the efficiency of magnetic separation, mixtures of CCRF-CEM and K562 cells pre-treated with UCNP–Apt–Biotin were added with IONP–Av at a concentration of 0.5 mg·mL^{-1} and incubated at room temperature for 30 min before being separated by a magnet for 10 min. Then, the separated cells were collected and re-dispersed in 100 μL of PBS, imaged and analyzed according to the above mentioned method. The separated cells were also directly loaded on glass slides and observed under a laser scanning confocal microscope (Leica SP5II) equipped with a 980-nm external laser.

2.8 Cell capture efficiency and cell viability

To study the capture efficiency, 10, 30, 100, 200 and 300 CCRF-CEM cells in 500 μL PBS were prepared and subsequently labeled with UCNP–Apt–Biotin and then MNP–Av. After magnetic separation, the captured cells in each sample were counted under the confocal microscopy.

To determine the viability of capture cells, two fluorescent dyes, calcein-AM and propidium iodide (PI) (Invitrogen), which emit green and red fluorescence, were used to label live and dead cells, respectively. 1,000 CCRF-CEM cells after labeling and separation by our method was co-stained by calcein-AM (0.003 mg·mL^{-1}) and PI (0.001 mg·mL^{-1}) for 15 min and then imaged by a Olympus IX71 CRiNuance fluorescence microscope.

2.9 Detection of tumor cells

For tumor cell detection, 0, 10, 50, 100, 500 and 1,000 CCRF-CEM cells spiked into 106 K562 cells in 500 μL PBS or FBS were incubated with UCNP–Apt–Biotin (0.2 mg·mL^{-1}) at 4 ℃ for 2 h. Then, the cells were washed to remove excess UCNPs. Afterwards, the cells were re-suspended in 500 μL PBS and incubated with IONPs–Av (0.5 mg·mL^{-1}) at 4 ℃ for 0.5 h. The cells were washed with PBS to remove nanoparticles and then separated with a magnet in a 1.5-mL tube. Finally, the obtained cells were re-suspended in 100 μL PBS and imaged as aforementioned.

For detection of tumor cells in blood, we spiked desired numbers of CCRF-CEM cells (0, 10, 100 and 1,000) into 500 μL of whole blood. The cell labeling, magnetic separation, and detection were carried following the same procedure as described above.

2.10 Immunofluorescence identification

Cells separated in the sample with 1,000 CCRF-CEM cells/500 μL whole blood were collected for immunofluorescence staining to confirm the UCL signals detected resulted from the specific recognition between PTK7 and the aptamer (Scg8). We used Rabbit polyclonal anti-colon carcinoma kinase-4 (CCK4) antibody and Cy3-conjugated Affinipure Goat-anti-Rabbit IgG to identify PTK7 positive CCRF-CEM cells. Cells were fixed with PBS containing 4% paraformaldehyde for 20 min at room temperature. After washing, cells were blocked with 0.5 mL of 5% bovine serum albumin (BSA) for 0.5 h and then washed with PBS. Antibodies at the concentration of 20 μg·mL^{-1} were

used for staining. The primary antibody staining needed 1 h at 37 ˚C in 0.5 mL of 1% BSA. After cells were washed five times with PBS, the secondary antibody staining was carried out for 45 min at 37 ˚C. Then cells were washed three times with PBS before diamidinophenylindole (DAPI) staining.

3 Results and discussion

$NaYF_4$(Yb:Er) UCNPs were synthesized following a well-established literature protocol [29]. Transmission electronic microscopy (TEM) images revealed that our UCNPs were monodisperse hexagonal nanocrystals (Fig. 1(b)). An amphiphilic polymer, C_{18}PMH–PEG–NH_2, was synthesized following our previously reported method and used to functionalize the as-made UCNPs. UCNP-PEG-NH_2 became water-soluble and were able to emit strong green light under 980-nm laser excitation (Fig. 1(c)). A thiolated aptamer targeting PTK-7 over-expressed on a variety of cancer cells [34, 35], together with biotin molecules, were co-conjugated to UCNPs (see the Electronic Supplementary Material (ESM) for detailed conjugation procedures), obtaining UCNP–Apt–Biotin to be used for tumor cell recognition.

Fe_3O_4 magnetic nanocrystals were synthesized by a classical procedure [32]. The MNPs showed uniform sizes at ~8 nm as revealed by TEM imaging (Fig. 1(d)). To make them water soluble, DMSA was used to functionalize the as-made Fe_3O_4 nanocrystals. The resulting water-soluble MNPs with carboxyl groups on their surface [31] were then conjugated with Av via amide formation, obtaining MNP–Av probes which were able to specifically bind with biotinylated UCNPs.

With both UCNP–Apt–Biotin and MNP–Av nanoprobes, we then designed a strategy for tumor cell capture and detection. As illustrated in Fig. 1(a), UCNP–Apt–Biotin nanoparticles were first introduced into a suspension of negative cells containing a small number of positive cancer cells, which will be specifically recognized by the aptamer conjugated on UCNPs. After removal of excess nanoparticles, the cells were then incubated with MNP–Av nanoparticles to allow capture of UCNPs anchored on positive cancer cells by MNPs. Finally, the cells were washed to remove free nanoparticles again and then separated by a magnet, which is able to capture positive cancer cells from a large pool of negative cells. Utilizing the UCL signals of UCNPs, we can then determine the number of positive tumor cells in the tested sample.

Thereafter, we first evaluated the cell binding specificity of UCNP–Apt–Biotin nanoprobes. PTK-7 positive CCRF-CEM cells or negative K562 cells [33, 34] were incubated with UCNP–Apt–Biotin, washed with PBS, and then observed under a laser scanning confocal microscope (LSCM) equipped with an 980-nm laser for UCL imaging. As expected, strong UCL signals were noticed on PTK-7 positive CCRF-CEM cells but not on the negative K562 cells (Figs. 2(a) and 2(b)). Different numbers of cells in 1.5-mL tubes were then imaged under an *in vivo* optical imaging system under 980-nm excitation. It was found that the UCL signals of CCRF-CEM cells increased as the number of cells increased (Fig. 2(d)). However, a low but appreciable level of non-specific binding of UCNPs was also noted on negative K562 cells, especially at the high cell numbers. The effect of UCNP–Apt–Biotin incubation time to the labeling efficiency was studied and optimized to be 2 h (Fig. S1 in the ESM).

Magnetic separation was then conducted by adding MNP–Av into the above cell samples pre-treated with UCNP–Apt–Biotin. When a mixture CCRF-CEM and K562 cells in a cell culture dish was placed nearby a magnet, under a confocal microscope, we found that cells positively labeled with UCNPs moved rapidly towards the direction of the applied magnetic field (Fig. 2(c)), while the other negative cells remained unmoved. Interestingly, while the majority of positive CCRF-CEM cells were captured by the magnet after subsequently incubating with UCNP–Apt–Biotin and MNP–Av, few negative cells were attracted by the applied magnetic field, despite the certain degree of non-specific binding of UCNPs on those cells (Fig. 2(d)). As the result, the magnetic separation with the help of MNP–Av was able to further reduce the non-specific signals of the negative cells (Fig. 2(e)), which is useful for improving the detection sensitivity of positive cells specifically recognized by the aptamer, especially in the presence of a huge of number of negative cells.

The above phenomenon can be attributed to the ultra-small sizes of MNPs used in this work. Unlike

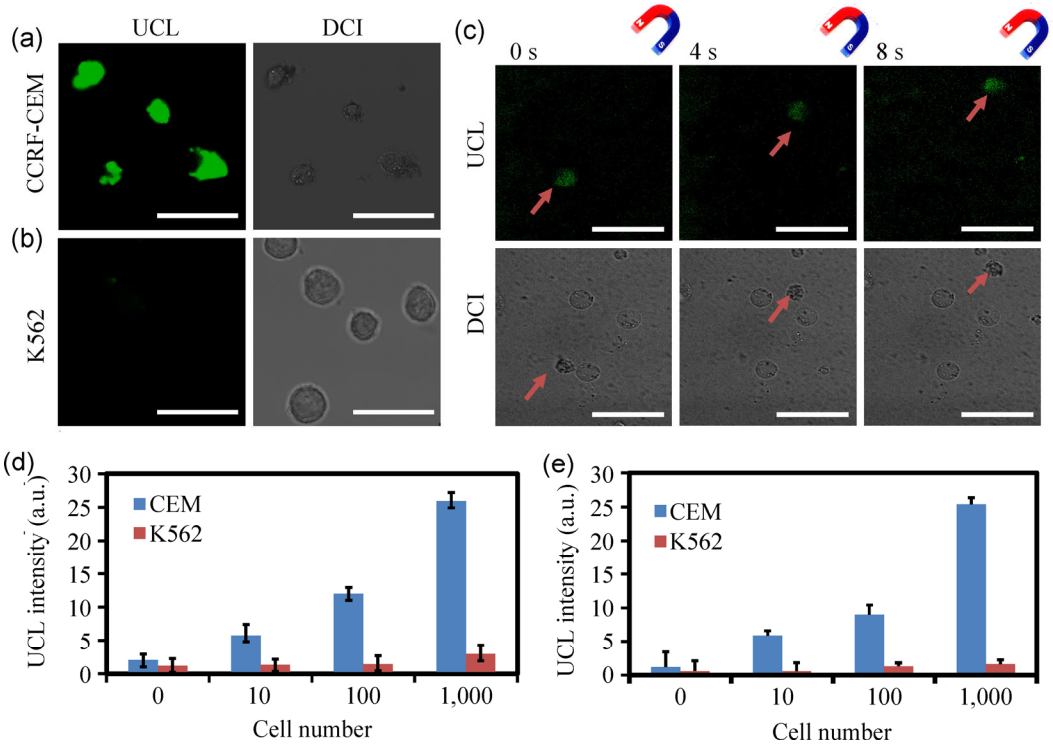

Figure 2 Specific recognition of CCRE-CEM cells by UCNP–Apt–Biotin nanoprobes. Confocal microscope images of CCRF-CEM cells (a) and K562 cells (b) after being incubated with APT-UCNPs (left: UCL fluorescence images; right: bright field images). (c) Confocal video images showing the cell movement in the process of magnetic separation. A mixture of CCRE-CEM and K562 cells was used in this experiment. The scale bars are 50 μm in the above images. UCL fluorescence intensities of designated numbers of CCRF-CEM cells and K562 cells detected without (d) and with (e) magnetic separation.

conventional magnetic beads with large sizes, which are rapidly attracted by the applied magnetic field, the ultra-small superparamagnetic MNPs monodispersed in the aqueous solution showed rather slow response to the external magnetic field (Fig. S2 in the ESM). In our system, a positive tumor cell has many attached UCNPs, each of which is further bound with multiple MNPs. By virtue of the large numbers of MNPs clustered on the surface of positive tumor cells, the accumulated magnetic force enables the instant response of the labeled cancer cells under the magnetic field. On the other hand, although a small number of UCNPs bind with negative cells as a result of non-specific binding—which is unavoidable—the total number of MNPs on each negative cell may not be large enough to allow the effective magnetic attraction of those cells. These effects taken together significantly reduce the non-specific signals during tumor cell detection.

With the optimized cell capture conditions, we then studied the cell capture efficiency using our method. Different numbers of CCRF-CEM cells in 500 μL of PBS were labeled subsequently with UCNP–Apt–Biotin and MNP–Av, and then separated by the magnet. The numbers of captured cells were counted under a microscope. Notably, the cell capture efficiencies reached ~80%–90% for all the samples (Fig. 3(a)). Moreover, the measured UCL intensity and the number of captured cells showed a reasonably good linear relationship, allowing us to use UCL imaging as a rapid and convenient method to estimate the number of captured tumor cells (Fig. 3(b)). Fluorescence images of captured cells after Calcein–AM/PI co-staining further revealed that the majority (~83%) of cells remained viable after labeling and separating by our method (Fig. 3(c)). Therefore, our strategy shows high cell capture efficiency without significant damage to the captured cells, making it promising for CTC detection and isolation.

We next wanted to use this strategy to detect CCRF-CEM tumor cells spiked in a large number of K562 cells. Various numbers of CCRF-CEM cells (10,

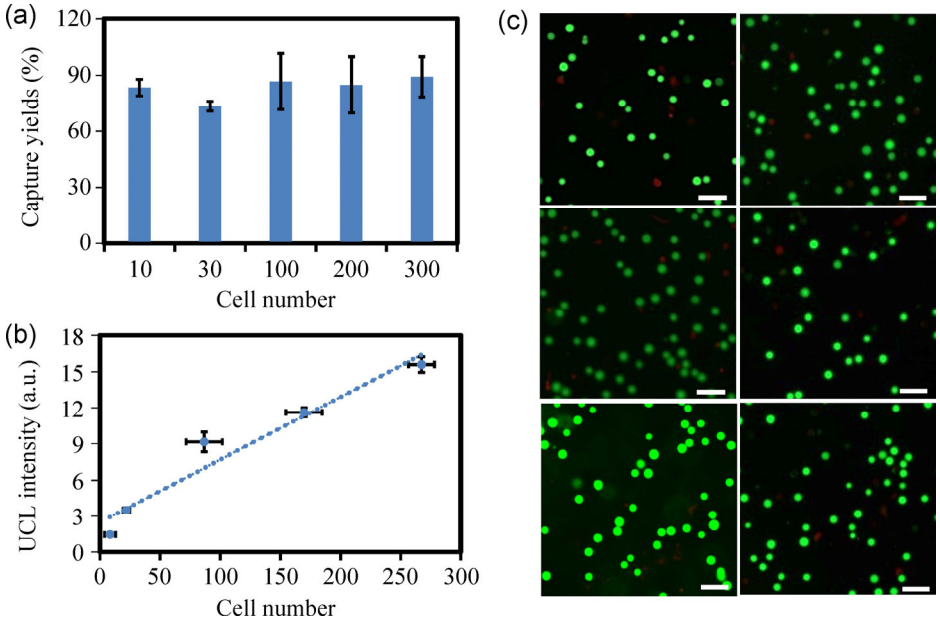

Figure 3 Capture efficiency and viability of cells isolated by our method. (a) Cell capture efficiencies of 10, 30, 100, 200 and 300 CCRF-CEM cells isolated under our optimal cell capture condition. (b) The relationship between UCL intensity and the number of captured cells. (c) Fluorescent images of captured CCRF-CEM cells by this method after calcein-AM (green, live cells) and PI (red, dead cells) co-staining. The majority of cells remained viable after labeling and isolation. Scale bar = 50 μm.

50, 100, 500 and 1,000) were mixed with 10^6 K562 cells in PBS or FBS solutions, and then subsequently incubated with UCNP–Apt–Biotin and MNP–Av nanoprobes. UCL signals of the samples after magnetic separation were then measured. It was found that as few as 10 CCRF-CEM cells spiked into 106 K562 cells suspended in either PBS or FBS could be detected by their UCL signals after magnetic separation using our approach (Figs. 4(a) and 4(c)). We also checked the interference of negative cell numbers in our method by mixing 100 CCRF-CEM cells with different numbers of K562 cells in either PBS or FBS. The same procedure was carried out to capture and detect positive CCRF-CEM cells in these samples. Importantly, an increase in negative cell numbers showed little effect on the signals of positive tumor cells after magnetic separation (Figs. 4(b) and 4(d)).

To demonstrate the possibility of our novel strategy for future detection of CTCs in real clinical samples, we spiked different numbers of CCRF-CEM cells into 0.5 mL of whole blood donated from a healthy volunteer to mimic patient blood samples. After sequentially incubating the blood samples with UCNP–Apt–Biotin and MNP–Av nanoprobes and followed by magnetic separation using the above procedures, the UCL signals of the separated samples were analyzed. As expected, the UCL signals increased with the increasing number of tumor cells present in the samples (Figs. 5(a) and 5(b)). More remarkably, as few as 10 CCRF-CEM cells spiked into 0.5 mL of whole blood were clearly detected by our method, demonstrating the great promise of this technique for future detection of CTCs in real patient samples.

The above captured tumor cells were further analyzed under a confocal microscope. The majority of captured cells showed strong UCL signals under the confocal microscope (Fig. 5(c)). To further confirm the captured cells were indeed positive tumor cells, immunofluorescence staining was then carried out. Apart from being able to be specifically recognized by Scg 8 aptamer, PTK7, also known as CCK4, can serve as the target of anti-CCK4 antibodies during immunofluorescence staining. As Scg 8 aptamer and anti-CCK4 antibody have different binding sites on PTK7, there should be no competition between UCNP–Apt–Biotin and anti-CCK4 when labeling CCRF-CEM cells [36]. Under the confocal microscope, it was found that most of the captured cells were indeed positive in both UCL signals and CCK4 expression (Fig. 5(d)), demonstrating the high specificity of our

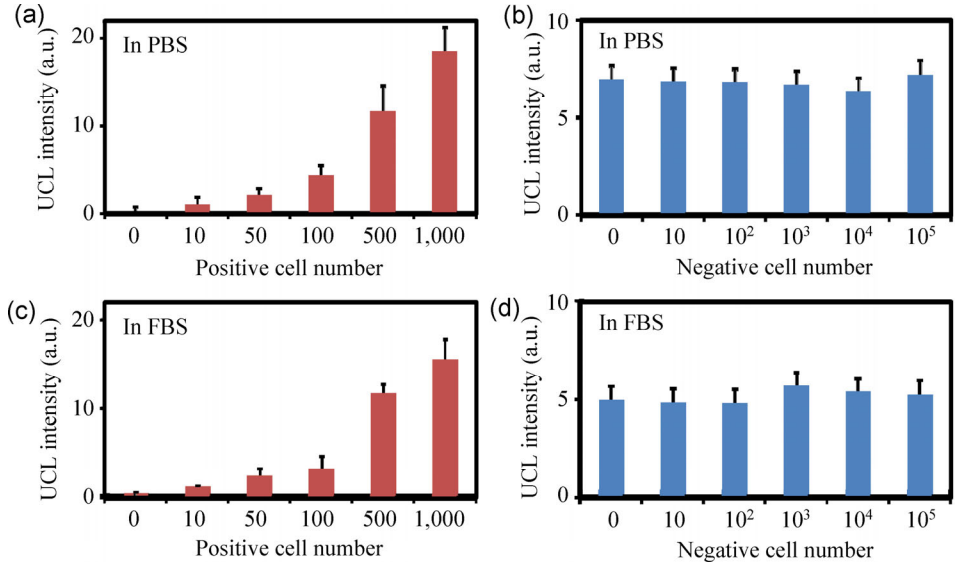

Figure 4 Detection of tumor cells in solutions. UCL fluorescence intensities of different numbers of CCRF-CEM cells spiked into 10^6 K562 cells in PBS (a) or FBS (c) after magnetic separation. UCL fluorescence intensities of 100 CCRF-CEM cells isolated from different numbers of K562 cells in PBS (b) or FBS (d) after magnetic separation.

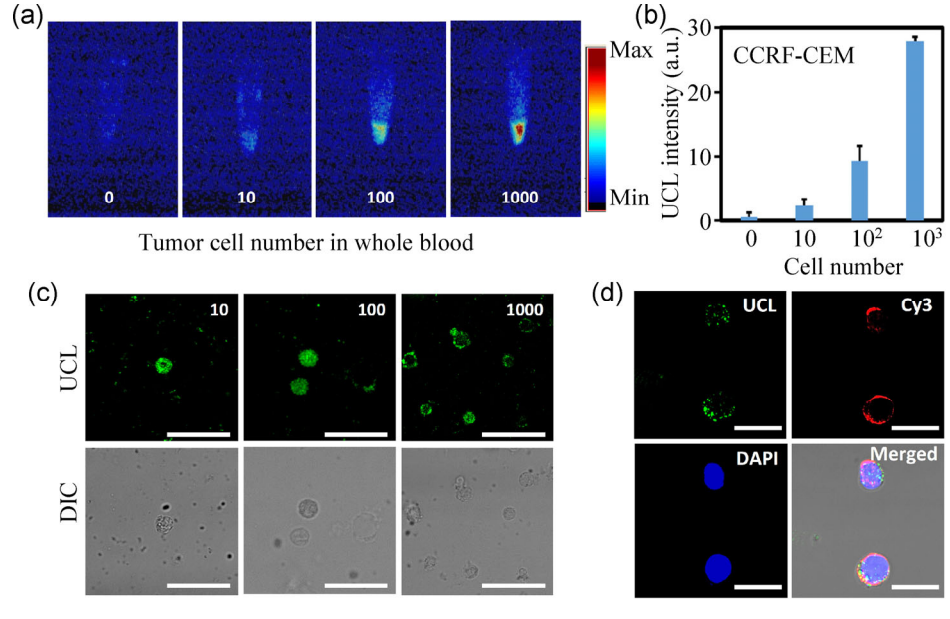

Figure 5 Tumor cell detection in whole blood samples. UCL images (a) and quantified signals (b) of whole blood samples spiked with different numbers of CCRF-CEM cells after magnetic separation. (c) Confocal images of isolated cells from samples in (a). Scale bar = 50 μm. (d) Immunofluoresence staining images of isolated cells from the sample containing 1,000 CCRF-CEM cells. Most of the collected cells were positive in both UCL signals from UCNPs and Cy3 signals from anti-CCK4. Scale bar = 25 μm.

tumor cell isolation and detection method. The purities of captured cells were found to be 70% ± 10%, 84% ± 7%, and 89% ± 7%, for blood samples containing 10, 100 and 1,000 tumor cells. Therefore, our method not only allows sensitive detection of tumor cells in the presence of a large number of negative cells or whole blood, but is also able to separate these positive tumor cells for further analysis, which is useful for future CTC research.

4 Conclusion

An easy and sensitive tumor cell detection and separation method based on magnetic separation and

UCL imaging has been developed by using tumor cell specific aptamer- and biotin-co-conjugated UCNPs, together with avidin-modified MNPs. Our strategy has several potential advantages: (1) The aptamer exploited in our approach is easily available and more stable than commonly used antibodies; (2) the UCNPs used in this method make our approach more promising for CTC detection than other methods based on dye-doped fluorescent nanoparticles or quantum dots, owing to the excellent photostability and autofluorescence-background-free feature of UCNPs; (3) the introduction of magnetic separation has been found to be effective not only for CTC isolation, but also in eliminating the non-specific signals of negative cells, which can be a major problem that limits the sensitivity of CTC detection. As the results, highly sensitive detection of as few as 10 tumor cells spiked into whole blood has been realized. Moreover, the captured cells could be easily collected for further careful analysis. Our approach may be a promising strategy for convenient and sensitive CTC detection and separation with high specificity and sensitivity, and shows great potential for future use in clinical diagnosis of cancer.

Acknowledgements

This work is supported by the National Basic Research Program of China (973 Program) (Nos. 2012CB932600 and 2011CB911000), the National Natural Science Foundation of China (Nos. 51222203, 51302180 and 31300824), the China Postdoctoral Science Foundation (Nos. 2013M530267 and 2013M531400), and a Project Funded by the Priority Academic Program Development of Jiangsu Higher Education Institutions.

Electronic Supplementary Material: Supplementary material (data regarding optimization of cell labeling conditions, and photos of a MNP–Av solution nearby a magnet) is available in the online version of this article at http://dx.doi.org/10.1007/s12274-014-0497-9.

References

[1] Ghossein, R. A.; Carusone, L.; Bhattacharya, S. Review: Polymerase chain reaction detection of micrometastases and circulating tumor cells: Application to melanoma, prostate, and thyroid carcinomas. *Diagn. Mol. Pathol.* **1999**, *8*, 165–175.

[2] Wittekind, C.; Neid, M. Cancer invasion and metastasis. *Oncology* **2005**, *69 (Suppl. 1)*, 14–16.

[3] Alunni-Fabbroni, M.; Sandri, M. T. Circulating tumour cells in clinical practice: Methods of detection and possible characterization. *Methods* **2010**, *50*, 289–297.

[4] Allard, W. J.; Matera, J.; Miller, M. C.; Repollet, M.; Connelly, M. C.; Rao, C.; Tibbe, A. G. J.; Uhr, J. W.; Terstappen, L. W. M. M. Tumor cells circulate in the peripheral blood of all major carcinomas but not in healthy subjects or patients with nonmalignant diseases. *Clin. Cancer Res.* **2004**, *10*, 6897–6904.

[5] Maltez-da Costa, M.; de la Escosura-Muñiz, A.; Nogués, C.; Barrios, L.; Ibáñez, E.; Merkoçi, A. Simple monitoring of cancer cells using nanoparticles. *Nano Lett.* **2012**, *12*, 4164–4171.

[6] Galanzha, E. I.; Shashkov, E. V.; Kelly, T.; Kim, J. W.; Yang, L.; Zharov, V. P. *In vivo* magnetic enrichment and multiplex photoacoustic detection of circulating tumour cells. *Nat. Nanotechnol.* **2009**, *4*, 855–860.

[7] Gazouli, M.; Lyberopoulou, A.; Pericleous, P.; Rizos, S.; Aravantinos, G.; Nikiteas, N.; Anagnou, N. P.; Efstathopoulos, E. P. Development of a quantum-dot-labelled magnetic immunoassay method for circulating colorectal cancer cell detection. *World J. Gastroenterol.* **2012**, *18*, 4419–4426.

[8] Zieglschmid, V.; Hollmann, C.; Böcher, O. Detection of disseminated tumor cells in peripheral blood. *Crit. Rev. Clin. Lab. Sci.* **2005**, *42*, 155–196.

[9] Park, G. S.; Kwon, H.; Kwak, D. W.; Park, S. Y.; Kim, M.; Lee, J. H.; Han, H.; Heo, S.; Li, X. S.; Lee, J. H. et al. Full surface embedding of gold clusters on silicon nanowires for efficient capture and photothermal therapy of circulating tumor cells. *Nano Lett.* **2012**, *12*, 1638–1642.

[10] Zhao, L. B.; Lu, Y. T.; Li, F. Q.; Wu, K.; Hou, S.; Yu, J. H.; Shen, Q. L.; Wu, D. X.; Song, M.; Ouyang, W. H. et al. High-purity prostate circulating tumor cell isolation by a polymer nanofiber-embedded microchip for whole exome sequencing. *Adv. Mater.* **2013**, *25*, 2897–2902.

[11] Chen, L.; Liu, X. L.; Su, B.; Li, J.; Jiang, L.; Han, D.; Wang, S. T. Aptamer-mediated efficient capture and release of T lymphocytes on nanostructured surfaces. *Adv. Mater.* **2011**, *23*, 4376–4380.

[12] Wang, S. T.; Liu, K.; Liu, J.; Yu, Z. T. F.; Xu, X. W.; Zhao, L. B.; Lee, T.; Lee, E. K.; Reiss, J.; Lee, Y. K. et al. Highly efficient capture of circulating tumor cells by using nanostructured silicon substrates with integrated chaotic micromixers. *Angew. Chem. Int. Ed.* **2011**, *50*, 3084–3088.

[13] Wu, L.; Wang, J. S.; Ren, J. S.; Qu, X. G. Ultrasensitive

telomerase activity detection in circulating tumor cells based on DNA metallization and sharp solid-state electrochemical techniques. *Adv. Funct. Mater.* **2014**, *24*, 2727–2733.

[14] Chang, Y. S.; di Tomaso, E.; McDonald, D. M.; Jones, R.; Jain, R. K.; Munn, L. L. Mosaic blood vessels in tumors: Frequency of cancer cells in contact with flowing blood. *Proc. Natl. Acad. Sci. USA* **2000**, *97*, 14608–14613.

[15] Auzel, F. Upconversion and anti-stokes processes with f and d ions in solids. *Chem. Rev.* **2004**, *104*, 139–174.

[16] Deng, M. L.; Ma, Y. X.; Huang, S.; Hu, G. F.; Wang, L. Y. Monodisperse upconversion $NaYF_4$ nanocrystals: Syntheses and bioapplications. *Nano Res.* **2011**, *4*, 685–694.

[17] Idris, N. M.; Gnanasammandhan, M. K.; Zhang, J.; Ho, P. C.; Mahendran, R.; Zhang, Y. *In vivo* photodynamic therapy using upconversion nanoparticles as remote-controlled nanotransducers. *Nat. Med.* **2012**, *18*, 1580–1585.

[18] Wang, C.; Cheng, L.; Liu, Z. Drug delivery with upconversion nanoparticles for multi-functional targeted cancer cell imaging and therapy. *Biomaterials.* **2011**, *32*, 1110–1120.

[19] Cheng, L.; Yang, K.; Zhang, S.; Shao, M. W.; Lee, S.; Liu, Z. Highly-sensitive multiplexed *in vivo* imaging using pegylated upconversion nanoparticles. *Nano Res.* **2010**, *3*, 722–732.

[20] Yang, Y. M.; Shao, Q.; Deng, R. R.; Wang, C.; Teng, X.; Cheng, K.; Cheng, Z.; Huang, L.; Liu, Z.; Liu, X. G. *In vitro* and *in vivo* uncaging and bioluminescence imaging by using photocaged upconversion nanoparticles. *Angew. Chem. Int. Ed.* **2012**, *51*, 3125–3129.

[21] Zhou, L.; Li, Z. H.; Liu, Z.; Yin, M. L.; Ren, J. S.; Qu, X. G. One-step nucleotide-programmed growth of porous upconversion nanoparticles: Application to cell labeling and drug delivery. *Nanoscale.* **2014**, *6*, 1445–1452.

[22] Yang, Y. Upconversion nanophosphors for use in bioimaging, therapy, drug delivery and bioassays. *Michromchim. Acta* **2014**, *181*, 263–294.

[23] Chen, F.; Bu, W. B.; Cai, W. B.; Shi, J. L. Engineering upconversion nanoparticles for biomedical imaging and therapy. In *Engineering in Translational Medicine*. Cai, W., Eds.; Springer: London, 2014; pp. 585–609.

[24] Xiong, L. Q.; Chen, Z. G.; Tian, Q. W.; Cao, T. Y.; Xu, C. J.; Li, F. Y. High contrast upconversion luminescence targeted imaging *in vivo* using peptide-labeled nanophosphors. *Anal. Chem.* **2009**, *81*, 8687–8694.

[25] He, L.; Feng, L. Z.; Cheng, L.; Liu, Y. M.; Li, Z. W.; Peng, R.; Li, Y. G.; Guo, L.; Liu, Z. Multilayer dual-polymer-coated upconversion nanoparticles for multimodal imaging and serum-enhanced gene delivery. *ACS Appl. Mater. Interface* **2013**, *5*, 10381–10388.

[26] Zvyagin, A. V.; Song, Z.; Nadort, A.; Sreenivasan, V. K. A.; Deyev, S. M. Luminescent nanomaterials for molecular-specific cellular imaging. In *Handbook of Nano-Optics and Nanophotonics*. Ohtsu, M., Eds.; Springer: Berlin Heidelberg, 2013; pp. 563–596.

[27] Wang, C.; Cheng, L.; Xu, H.; Liu, Z. Towards whole-body imaging at the single cell level using ultra-sensitive stem cell labeling with oligo-arginine modified upconversion nanoparticles. *Biomaterials.* **2012**, *33*, 4872–4881.

[28] Cheng, L.; Wang, C.; Ma, X. X.; Wang, Q. L.; Cheng, Y.; Wang, H.; Li, Y. G.; Liu, Z. Multifunctional upconversion nanoparticles for dual-modal imaging-guided stem cell therapy under remote magnetic control. *Adv. Funct. Mater.* **2013**, *23*, 272–280.

[29] Liu, C. H.; Wang, H.; Li, X.; Chen, D. P. Monodisperse, size-tunable and highly efficient β-$NaYF_4$:Yb, Er (Tm) upconversion luminescent nanospheres: Controllable synthesis and their surface modifications. *J. Mater. Chem.* **2009**, *19*, 3546–3553.

[30] Prencipe, G.; Tabakman, S. M.; Welsher, K.; Liu, Z.; Goodwin, A. P.; Zhang, L.; Henry, J.; Dai, H. PEG branched polymer for functionalization of nanomaterials with ultralong blood circulation. *J. Am. Chem. Soc.* **2009**, *131*, 4783–4787.

[31] Wang, C.; Ma, X. X.; Ye, S. Q.; Cheng, L.; Yang, K.; Guo, L.; Li, C. H.; Li, Y. G.; Liu, Z. Protamine functionalized single-walled carbon nanotubes for stem cell labeling and *in vivo* Raman/magnetic resonance/photoacoustic triple-modal imaging. *Adv. Funct. Mater.* **2012**, *22*, 2363–2375.

[32] Sun, S. H.; Zeng, H.; Robinson, D. B.; Raoux, S.; Rice, P. M.; Wang, S. X.; Li, G. X. Monodisperse MFe_2O_4 (M = Fe, Co, Mn) nanoparticles. *J. Am. Chem. Soc.* **2004**, *126*, 273–279.

[33] Lee, H.; Yoon, T. J.; Figueiredo, J. L.; Swirski, F. K.; Weissleder, R. Rapid detection and profiling of cancer cells in fine-needle aspirates. *Proc. Natl. Acad. Sci. USA* **2009**, *106*, 12459–12464.

[34] Smith, J. E.; Medley, C. D.; Tang, Z. W.; Shangguan, D.; Lofton, C.; Tan, W. H. Aptamer-conjugated nanoparticles for the collection and detection of multiple cancer cells. *Anal. Chem.* **2007**, *79*, 3075–3082.

[35] Herr, J. K.; Smith, J. E.; Medley, C. D.; Shangguan, D.; Tan, W. H. Aptamer-conjugated nanoparticles for selective collection and detection of cancer cells. *Anal. Chem.* **2006**, *78*, 2918–2924.

[36] Shangguan, D.; Cao, Z. H.; Meng, L.; Mallikaratchy, P.; Sefah, K.; Wang, H.; Li, Y.; Tan, W. H. Cell-specific aptamer probes for membrane protein elucidation in cancer cells. *J. Proteome Res.* **2008**, *7*, 2133–2139.